INTERPRETATION OF ELECTROCHEMICAL NOISE PARAMETERS AS INDICATORS OF INITIATION AND PROPAGATION OF SCC OF AN ALLOY 600 SG TUBE AT HIGH TEMPERATURES

SUNG-WOO KIM* and HONG-PYO KIM
Korea Atomic Energy Research Institute
1045 Daedeok-Daero, Yuseong-Gu, Daejeon 305-353, Korea
*Corresponding author. E-mail : kimsw@kaeri.re.kr

Received April 6, 2009
Accepted for Publication August 10, 2009

The present article is concerned with the application of an electrochemical noise (EN) monitoring technique to analyze the initiation and propagation of Pb-assisted stress corrosion cracking (SCC) of an Alloy 600 material in a simulated environment of a steam generator (SG) sludge pile at high temperatures. A typical increase of electrochemical current noise (ECN) and electrochemical potential noise (EPN) was frequently recorded from the EN measurement in a caustic solution with such impurities as PbO and CuO, indicating that there are localized corrosion events occurring. With the aid of microscopic and spectral analyses, the EN data involving information on such stochastic processes as uniform corrosion and the initiation and propagation of SCC, were analyzed based on a stochastic theory.

KEYWORDS : Alloy 600, Electrochemical Noise, Electrochemical Current Noise, Electrochemical Potential Noise, Stress Corrosion Cracking, Steam Generator Tube

1. INTRODUCTION

Nickel-based alloys such as Alloy 600 and Alloy 690 have been used as the steam generator (SG) tubing material in a pressurized water reactor (PWR) due to their high corrosion resistance. However, many types of corrosion have occurred in highly caustic environments containing some oxidizing impurities, especially in SG sludge piles, because the highly caustic conditions can be developed in the heated crevices of the PWR's SG [1]. Among those impurities, Pb is well known to assist in stress corrosion cracking (SCC) of the SG tubing in caustic environments [2]. Many authors have reported on the cracking modes of SCC in Pb-contaminated solutions and the role of Pb on the passive films formed on nickel-based alloys to explain the mechanism of SCC [3-6].

Recently, there was an approach to investigate the mechanism by distinguishing between the initiation and propagation stages of Pb-assisted SCC using an electrochemical noise (EN) technique [7]. EN is defined as a fluctuation of the electrochemical potential or current which is observed experimentally to be associated with localized corrosion processes [8,9]. From the analyses of the EN parameters such as the frequency of events, the average charge of events, the noise resistance [10-12], and the mean free time-to-failure [7,13-15], various types of localized corrosion are distinguishable from each other. Therefore, the EN monitoring technique has become a useful tool for characterizing such localized corrosions as pitting corrosion, crevice corrosion, and SCC.

This work analyzes the EN generated during Pb-assisted SCC of Alloy 600 at high temperatures. The EN was measured from the Alloy 600 C-ring specimens in the highly caustic solution containing oxidizing impurities in two different ways: In a potentiostatic controlled current noise (PCCN) mode, the electrochemical current noise (ECN) was measured from the stressed C-ring specimen by applying an anodic potential. In an uncorrelated three electrode current and potential noise (UCPN) mode, the electrochemical potential noise (EPN) and the ECN were measured simultaneously from the stressed C-ring specimen. Changes in amplitude and time interval of the ECN and EPN, and variations in the power spectral density of the ECN and EPN were analyzed in terms of the initiation and propagation of Pb-assisted SCC of Alloy 600 in highly caustic solutions at high temperatures.

2. EXPERIMENTAL

2.1 Preparation of C-ring Specimens

Alloy 600 SG tubing (Valinox Heat No. NX8527) with a 22.23 mm outer diameter (OD) and 1.27 mm thickness was used for this work. The chemical composition of the materials is given in Table 1. The tubing was pilgered by the manufacturer, and heat treated in our laboratory at 920°C for 15 min in an Ar-filled quartz capsule in a furnace, followed by water quenching, to simulate low-temperature mill-annealing (LTMA). The C-ring specimens were fabricated from the Alloy 600 SG tubing in accordance with the ASTM G38 standard. The OD surface of the specimens was ground by #1000 emery paper, and then cleaned with ethanol and water in sequence. The C-ring specimen was stressed to 150% of its room temperature yield strength (YS) at the apex using an Alloy 600 bolt and nut.

2.2 Electrochemical Noise Measurement

The EN measurements were carried out with a Zahner IM6e equipped with a Zahner NProbe as described in detail in our previous report [7]. In the PCCN mode, only ECN was recorded between the stressed and unstressed specimens during the application of an anodic potential of 100 mV vs. open circuit potential (OCP). No information about the EPN was obtained in the PCCN mode. On the other hand, in the UCPN mode, the EPN of the stressed specimen was recorded relative to a reference electrode simultaneously with the ECN between the stressed and unstressed specimens at the OCP. The reference electrode was an external Ag/AgCl/KCl (0.1 M) electrode, specially designed and constructed for high temperature and pressure applications (Toshin-Kogyo Co., UH type). For reliable measurements of the electrochemical potential, the reference electrode was reassembled and recalibrated frequently during the interruption of the test series. The sample interval and the frequency bandwidth were 0.5 s and 1 mHz ~ 1 Hz, respectively. The power spectral density and the frequency of events were calculated from each set of time records that consisted of 2,048 data points acquired for 1×10^3 s.

Table 1. Chemical Composition of Alloy 600 Materials (wt%)

C	Mn	Si	P	S	Ni	Cr	Ti	Al	Co	Cu	Fe
0.024	0.23	0.13	0.005	<0.001	74.90	15.37	0.28	0.20	0.016	0.009	8.84

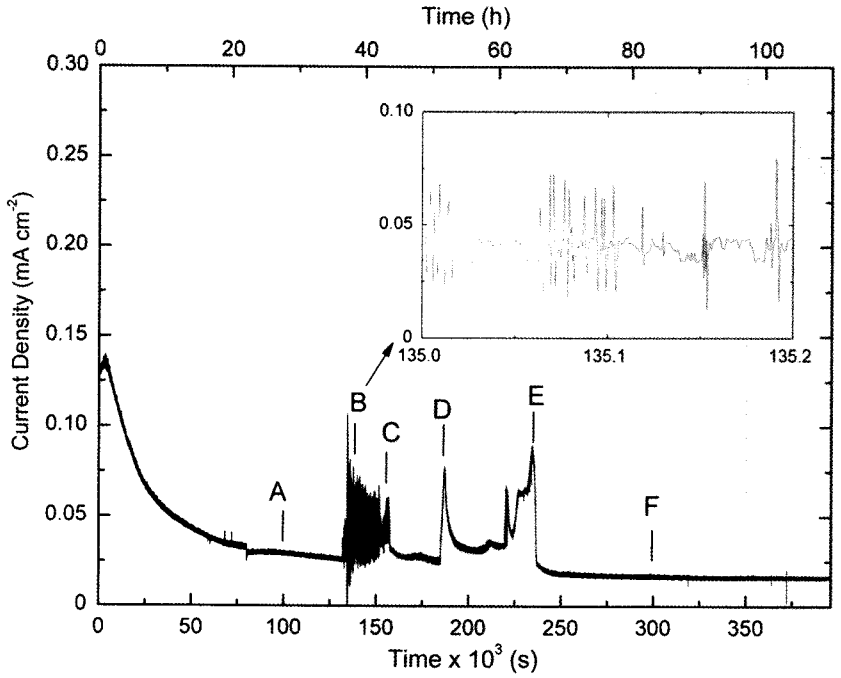

Fig. 1. Time Records of the ECN Measured in the PCCN Mode from the Stressed C-ring Specimens in a 40 wt% NaOH Solution Containing 0.01 wt% PbO at 315°C for 110 h. The Test was Interrupted and the Specimen Surface was Examined for Cracking at Accumulated Immersion Times of 22, 42, and 110 h

2.3 C-ring Immersion Tests

In the PCCN mode, the test environment was an aqueous solution of 40 wt% NaOH containing 0.01 wt% PbO (leaded caustic solution). Pb-assisted SCC was accelerated by the potentiostatic method by maintaining the electrochemical potential in the active-passive range for Alloy 600 in caustic environments [16]. The C-ring tests in the PCCN mode were performed at 315°C for 110 h.

In the UCPN mode, the tests were carried out in a leaded caustic solution, and that solution plus 500 ppm CuO. CuO was added to the leaded caustic solution to accelerate the Pb-assisted SCC. CuO is a well-known oxidizing species that increases the corrosion potential and promotes Pb-assisted SCC [1,16]. The C-ring tests in the UCPN mode were performed at 290°C for a total accumulated immersion time of 400 h, and consisted of two phases of immersions in sequence: (1) 278 h in the leaded caustic solution (40 wt% NaOH with 0.01 wt% Pb) and (2) 122 h in that solution plus 500 ppm CuO. The addition of CuO caused an increase of the electrochemical potential by about 150 mV. The surfaces of the specimens were intermittently examined for cracking using an optical stereo-microscopy and scanning electron microscopy (SEM, JEOL JSM-6360).

Prior to the immersion test, the test solution was deaerated with 99.99% nitrogen gas for 20 h. After the entire immersion test, the specimens were chemically etched with a solution of 2% bromine+98% methanol, and then examined by a SEM equipped with an energy dispersive spectrometer (EDS, Oxford-7582).

3. RESULTS AND DISCUSSION

3.1 Spectral Analysis of Electrochemical Noise in PCCN Mode

Fig. 1 gives the time record of the ECN measured from the stressed C-ring specimen in the leaded caustic solution at 315°C for 110 h by the EN technique in the PCCN mode. There were abrupt changes in the ECN after immersion for 132×10^3 s (points B, C, D, and E in Fig. 1), which have generally been observed during localized corrosions such as pitting corrosion, crevice corrosion, intergranular corrosion, and SCC [7-12]. As compared with the ECN at point A, the ECN revealed repetitive current rises followed by fast decay with certain time intervals in the time record at points B and C (see the insert in Fig. 1). This means that discrete events of a localized corrosion are occurring from 132×10^3 to 158×10^3 s during the immersion in the leaded caustic solution. On the other hand, from 185×10^3 to 240×10^3 s, the ECN revealed current increases followed by slower decay with longer time intervals in the time record at points D and E, indicating the occurrence of a localized corrosion event inducing larger charge passages than that at points B and C.

In order to correlate the changes of the ECN with the cracking stages, the test was interrupted and the surface of the specimen was examined for cracking at accumulated immersion times of 22, 42, and 110 h. After the immersion test in the leaded caustic solution for 22 h, the extensive examination of the surface of the specimen ruled out any cracking. At the accumulated immersion time of 42 h, it turned out that there were many defect sites such as local break-down of the surface oxide film and micro-cracks initiated with depth of one grain boundary or less in the OD surface from the SEM analysis of the C-ring apex as shown in Fig. 2(a). After the entire immersion test of 110 h, one of the micro-cracks was propagated as presented in Fig. 2(b). The crack was propagated in an intergranular (IG) mode and the crack mouth and tip were covered by a surface oxide film, which is typical of SCC of Alloy 600 in leaded caustic environments [3-6]. The chemical composition of the surface film was analyzed with EDS,

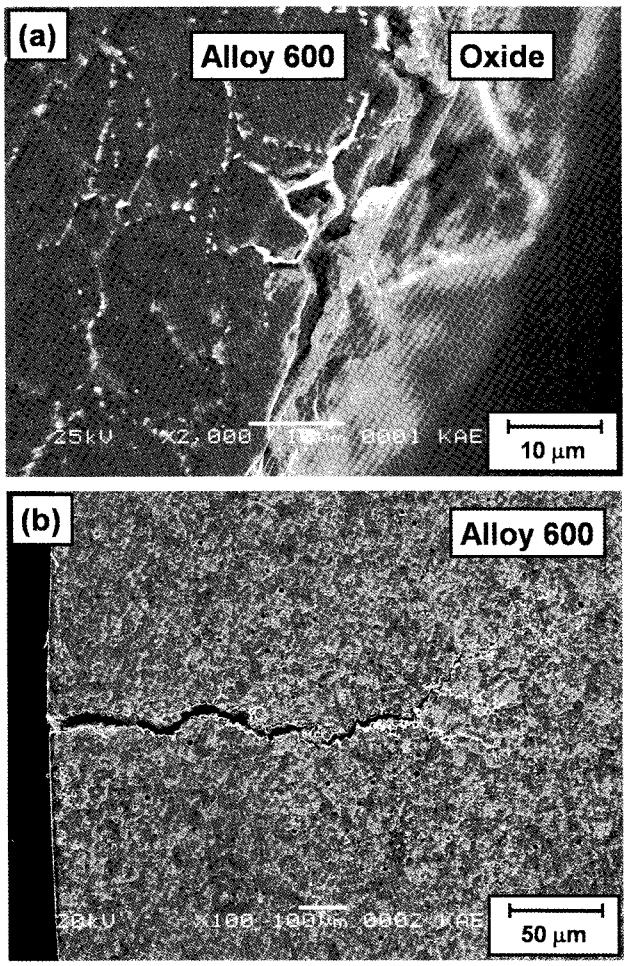

Fig. 2. SEM Micrographs of the Side Surface of the C-ring Apex after the Accumulated Immersion Times of (a) 42 h and (b) 110 h in the Leaded Caustic Solution at 315°C

Table 2. Chemical Composition of the Matrix and the Surface Film of the Crack Mouth and Tip after a Whole Immersion Test in 40 wt% NaOH Solution Containing 0.01 wt% PbO at 315°C for 110 h (wt%)

Position	O	Al	Ti	Cr	Mn	Fe	Ni
Matrix	ND	0.31	0.18	15.74	0.27	8.35	75.14
Crack mouth	21.61	0.34	0.11	5.96	0.15	2.65	69.18
Crack tip	22.04	0.21	0.15	8.88	0.05	4.10	64.57

ND: Not detectable.

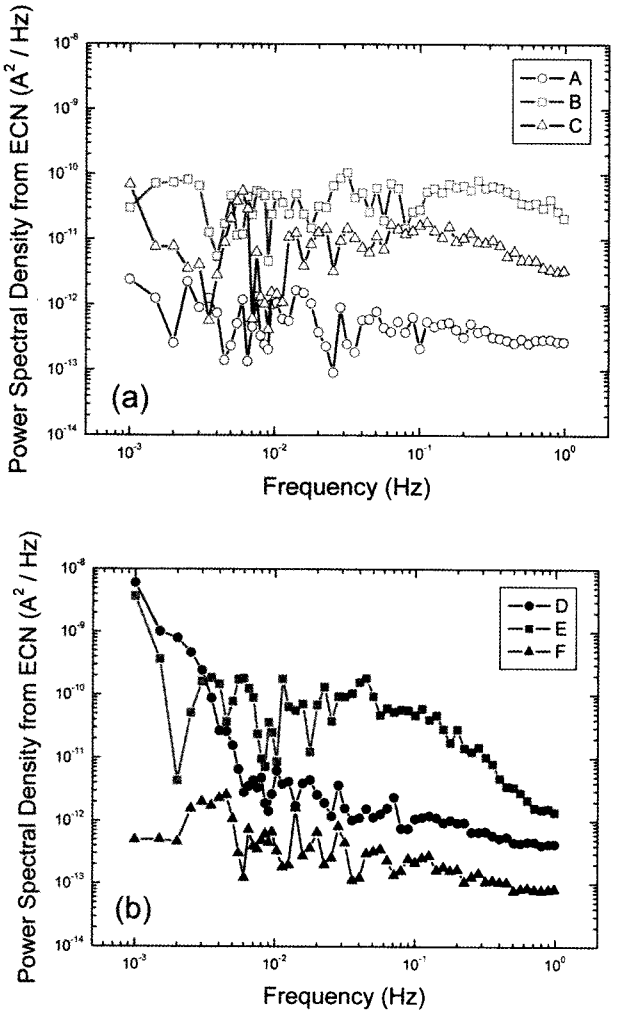

Fig. 3. Plots of the PSD vs. the Frequency Calculated from each Time Record of the ECN by the FFT Algorithm at Points (a) A, B, and C and (b) D, E, and F

and summarized in Table 2, along with the chemical composition of the Alloy 600 matrix.

With the aid of microscopic analysis, it is easily anticipated that the current rises followed by steeper decay with shorter time intervals in the time record of the ECN at points B and C in Fig. 1 are mainly due to the initiation of SCC, whereas the current increases followed by slower decay with longer time intervals in the time record at points D and E in Fig. 1 are attributable to its propagation.

Figs. 3(a) and (b) present the plots of the power spectral density (PSD) vs. the frequency calculated from each time record of the ECN by a fast Fourier transform (FFT) algorithm at points A, B, and C, and D, E, and F, respectively. In Fig. 3(a), it is clearly seen that the PSD of the ECN obtained at points B and C, where the initiation of SCC is expected to occur, is higher at whole frequency ranges than that obtained at point A, where the general corrosion (the formation of the passive oxide film) occurs on the C-ring surface. Similar behaviors were found in Fig. 3(b), that is, the PSD of the ECN obtained at points D and E, where the propagation of SCC is supposed to occur, is higher than that obtained at point F, except the remarkable increase of the PSD at a low frequency limit. The increases of the PSD especially at a low frequency limit in Figs. 3(a) and (b) strongly indicate the increase in the number of localized corrosion events, that is, the initiation and the propagation of Pb-assisted SCC, respectively, as previously reported [7]. Since the type of corrosion can not be reliably distinguished on the basis of the roll-off slope [10], it will not be considered as an indicator of localized corrosions in this work.

3.2 Spectral Analysis of Electrochemical Noise in UCPN Mode

Figs. 4(a) and (b) present typical EPN and ECN recorded from the stressed specimen in the leaded caustic solution for the time period from 982×10^3 to 996×10^3 s, and for that solution plus CuO for the time period from 1406×10^3 to 1420×10^3 s, respectively, by the EN measurement in the UCPN mode. There were typical current increases in the ECN concurrent with the potential drops in the EPN at points A, C, D, and F, which have also generally been observed during localized corrosions; the current increase corresponding to the potential decrease means a local breakdown of the oxide film resulting in an exposure and local dissolution of the metal surface, whereas the current decrease accompanied by the potential recovery indicates a repair of the surface oxide film (repassivation).

The ECN at points A and C in Fig. 4(a) revealed repetitive current increases followed by faster decay with

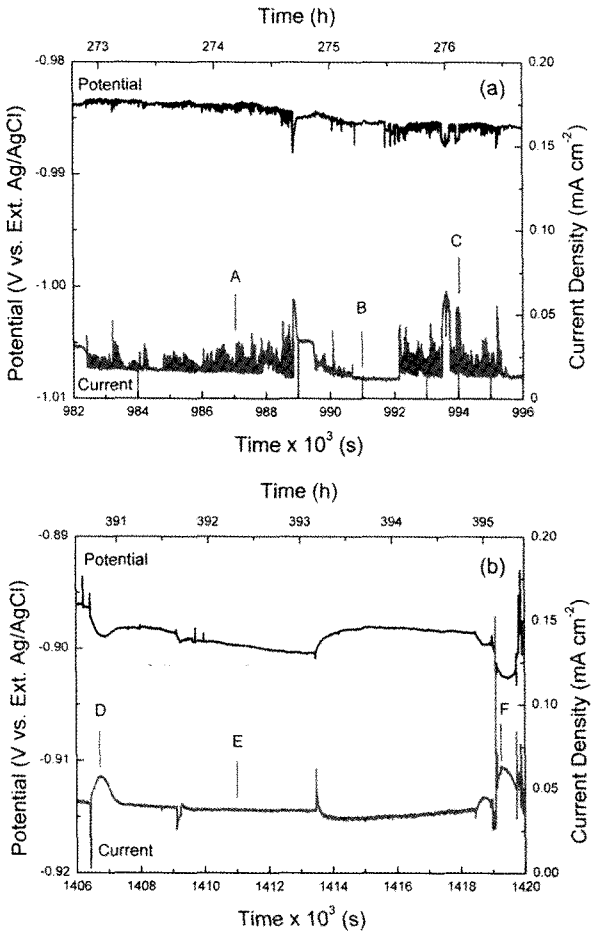

Fig. 4. Time Records of the EPN and the ECN Recorded in UCPN Mode (a) for the Leaded Caustic Solution for the Time Period from 980×10^3 to 996×10^3 s, and (b) for that Solution Plus CuO for the Time Period from 1405×10^3 to 1421×10^3 s at 290°C

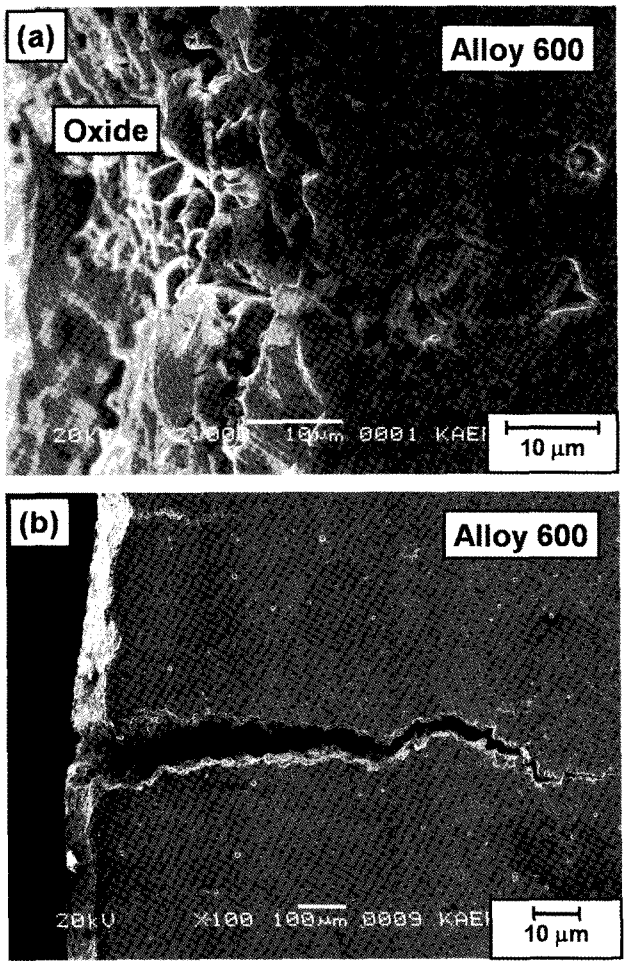

Fig. 5. SEM Micrographs of the Side Surface of the C-ring Apex after the Accumulated Immersion Times of (a) 278 h in the Leaded Caustic Solution and (b) 400 h in that Solution Plus CuO at 290°C

shorter time intervals when compared to the ECN at points D and F in Fig. 4(b) exhibiting more localized behavior, that is, current rises followed by slower decay with longer time intervals. It is notable that the behavior of the ECN at points A and C recorded in the UCPN mode (Fig. 4(a)) was fairly similar with that of the ECN at points B and C obtained in the PCCN mode (Fig. 1). Also, the ECN at points D and F in the UCPN mode (Fig. 4(b)) resembles the ECN at points D and E in the PCCN mode (Fig. 1) in appearance.

After the immersion test in the leaded caustic solution for 278 h, the surface of the specimen was extensively examined for cracking. From the SEM analysis, the local break-down of the surface oxide film and many defect sites were found on the surface of the stressed specimen (Fig. 5(a)). After the entire immersion test in the leaded caustic solution plus CuO for 400 h, several cracks were propagated in the IG mode (Fig. 5(b)). Consequently, it is strongly suggested that the current increases in the ECN accompanied by the potential drops in the EPN in Fig. 4(a) are mainly due to the initiation of SCC and those changes in the ECN and the EPN in Fig. 4(b) are attributable to its propagation.

Figs. 6(a) and (b) present the plots of the PSD vs. the frequency calculated from each time record of the ECN and the EPN, respectively, by the FFT algorithm at points A, B, and C in Fig. 4(a). It is obvious that the PSD of both ECN and EPN at points A and C, where SCC is expected to be initiated in the leaded caustic solution, is higher at whole frequency ranges than that obtained at point B where the general corrosion (the repassivation of the surface oxide film) occurs on the C-ring surface. Similar trends were observed in Figs. 7(a) and (b); the PSD of ECN and EPN at points D and F, where SCC is supposed to be propagated in the leaded caustic solution plus CuO, is higher than that obtained at point E. It is noticeable that the PSD of both ECN and EPN due to the propagation of

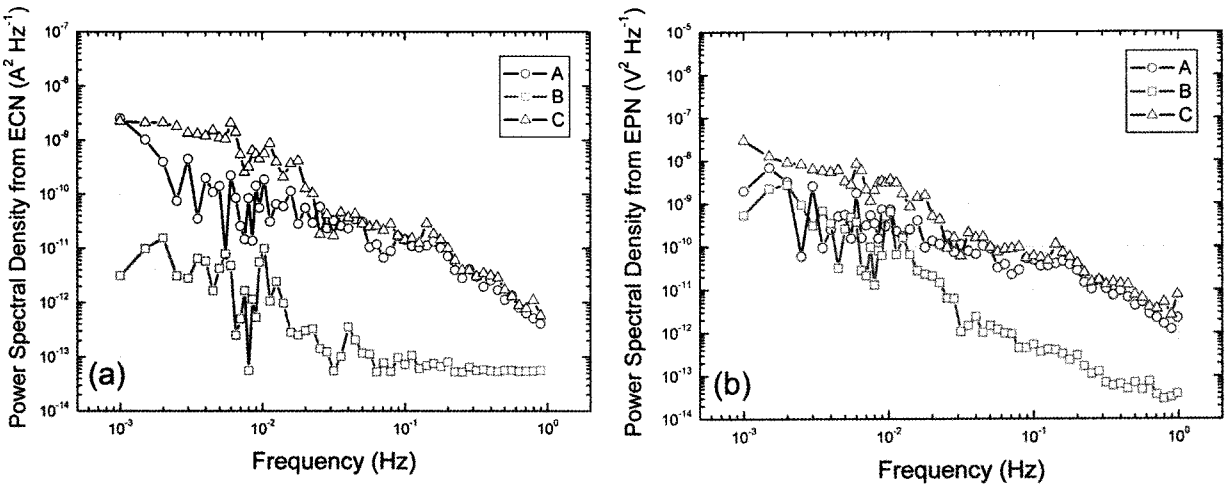

Fig. 6. Plots of the PSD vs. the Frequency Calculated from each Time Record of (a) the ECN and (b) the EPN by the FFT Algorithm at Points A, B, and C in Fig. 4(a)

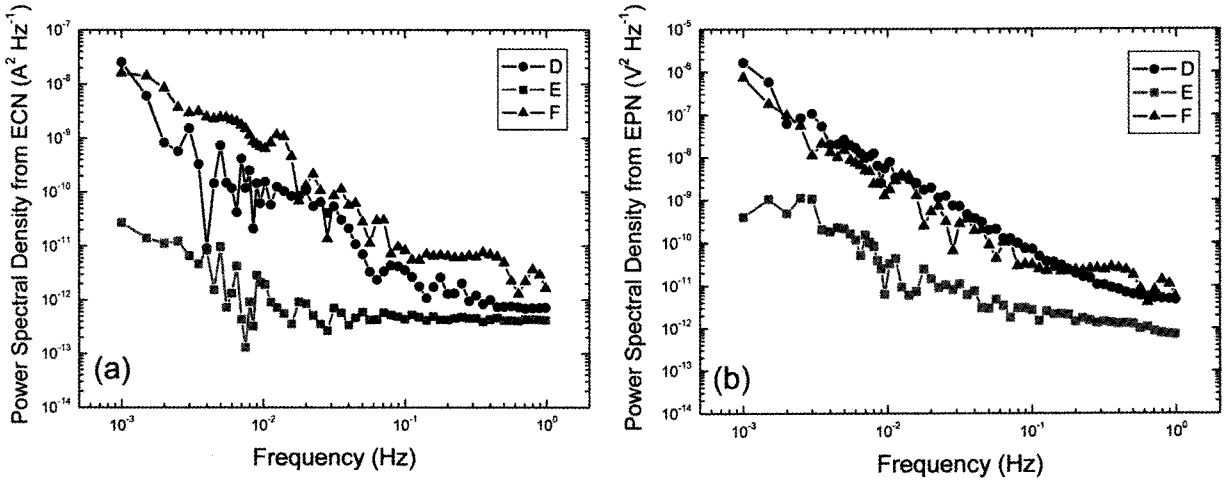

Fig. 7. Plots of the PSD vs. the Frequency Calculated from each Time Record of (a) the ECN and (b) the EPN by the FFT Algorithm at Points D, E, and F in Fig. 4(b)

SCC (Figs. 7(a) and (b)) revealed a more dominant increase at a low frequency limit as compared to that PSD due to the initiation of SCC (Figs. 6(a) and (b)), indicating more localized characteristics of the propagation of SCC. The results from the spectral analyses of the ECN and the EPN recorded in the UCPN mode coincided well with that obtained in the PCCN mode.

3.3 Stochastic Analysis of Electrochemical Noise

To evaluate the stochastic characteristics of the initiation and the propagation of SCC, a shot-noise analysis was employed in this work under the assumption that the ECN concurrent with the EPN is independently produced by the individual event of localized corrosions. Based on the shot-noise theory [10-12], the frequency of events f_n of the localized corrosions is determined from the time record of the EPN as given by,

$$f_n = B^2 / \Psi_E A \tag{1}$$

where, B is the Stern-Geary coefficient, Ψ_E is the PSD value of the EPN calculated by averaging several low-frequency points using the FFT algorithm, and A represents the exposed electrode area. From a set of f_n calculated from the PSD plots of the EPN according to Eq. (1), the cumulative probability $F(f_n)$ at each f_n is determined numerically by a mean rank approximation [10]. In this work, the probability of f_n for the Pb-assisted SCC was analyzed using the

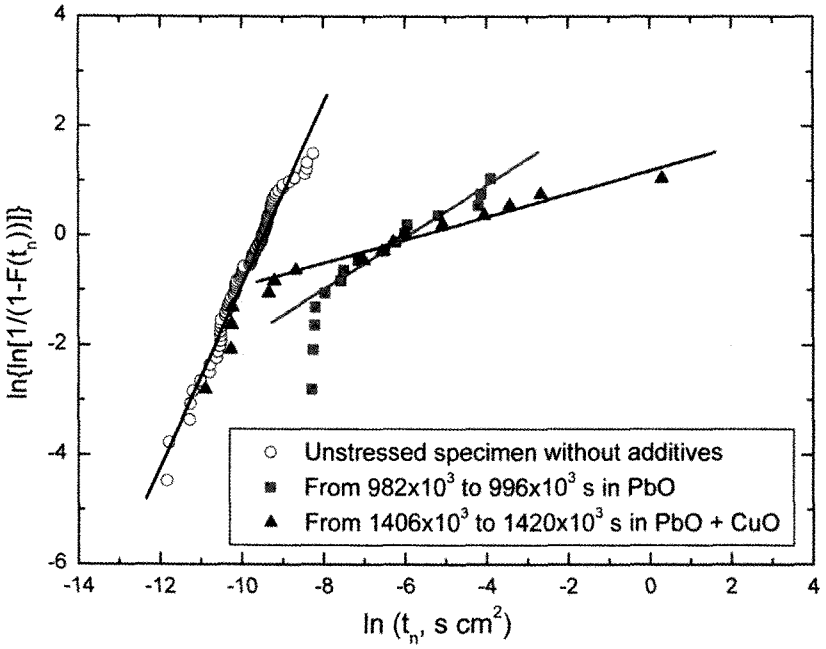

Fig. 8. Plots of $\ln\{\ln[1/(1-F(t_n))]\}$ vs. $\ln t_n$ Calculated from the Sets of f_n at the Same Time Period as Figs. 4(a) and (b). For a Comparison, the Probability of t_n Obtained from the EN Measurement of Two Identical Unstressed Alloy 600 Specimens in a 40 wt% NaOH Solution without Impurities at 290°C is also Plotted

Weibull distribution function, the most commonly used cumulative probability function for predicting the life and failure rate [13-15]. Using the Weibull distribution function, the probability of the mean time-to-failure, t_n, which corresponds to $1/f_n$, is expressed as,

$$\ln\{\ln[1/(1-F(t_n))]\} = m\ln t_n - \ln n \qquad (2)$$

where, m and n are the shape and scale parameters, respectively.

Fig. 8 demonstrates the plots of $\ln\{\ln[1/(1-F(t_n))]\}$ vs. $\ln t_n$ calculated from the sets of f_n at the same time period as Figs. 4(a) and (b). For a comparison, the probability of t_n obtained from the EN measurement of two identical unstressed Alloy 600 specimens in a 40 wt% NaOH solution without impurities at 290°C is also plotted. Only general corrosion occurred on the unstressed specimen surface without any cracking. In Fig. 8, it was easily anticipated that the mean time-to-failure t_n for the localized corrosions such as the initiation and the propagation of SCC shifted to a higher value, analogous to the shift of f_n to a lower frequency when compared to that for the general corrosion.

In our previous works [7,13,15], it was reported that the shape parameter m of the Weibull distribution can be regarded as an indicator of types of corrosion. In the present work, the value of m determined from Fig. 8 by a linear curve fitting method was 1.46 for the general corrosion on the unstressed specimen in the caustic solution without any oxidizing impurities, 0.47 for the initiation of SCC on the stressed specimen in the leaded caustic solution, and 0.21 for its propagation in the leaded caustic solution plus CuO. The values of m in this work revealed good agreement with those values previously reported for each stage of the Pb-assisted SCC [7].

4. CONCLUSIONS

From the microscopic and EN analyses of Alloy 600 SG tube materials in the leaded caustic solution environment at high temperatures, it is strongly suggested that the repetitive current rises followed by steeper decay with shorter time intervals in the time record of the ECN measured in the PCCN mode are mainly due to the initiation of SCC, whereas the current increases followed by slower decay with longer time intervals are attributable to its propagation. From the spectral analysis of the ECN, the PSD increased more remarkably at low frequency limits for the propagation of SCC as compared to that for the initiation of SCC. Similar trends were observed in both ECN and EPN measured in the UCPN mode in the caustic solution environments with various oxidizing impurities. In addition, from the stochastic analysis of the EPN obtained in the UCPN mode, it was found that the shape parameter of the Weibull distribution of the mean time-to-failure for the initiation of SCC is clearly distinguishable from that parameter for the propagation of SCC as well as for the general corrosion.

ACKNOWLEDGEMENT

This work was funded by the Korea Ministry of Education, Science and Technology.

REFERENCES

[1] R.J. Jacko, "Corrosion Evaluation of Thermally Treated Alloy 600 Tubing in Primary and Faulted Secondary Water Environments," EPRI NP-6721, Pittsburgh, Pennsylvania (1990).

[2] T. Sakai, S. Okabayashi, K. Aoki, K. Matsumoto and Y. Kishi, "A study of oxide thin film of Alloy 600 in high temperature water containing lead," *Corrosion/90*, paper no. 520, NACE, Houston (1990).

[3] S.S. Hwang, U.C. Kim and Y .S. Park, "The effects of Pb on the passive film of Ni-base alloy in high temperature water," *J. Nucl. Mater.*, **246**, 77 (1997).

[4] S.S. Hwang, H.P. Kim, D.H. Lee, U.C. Kim and J.S. Kim, "The mode of stress corrosion cracking in Ni-base alloys in high temperature water containing lead," *J. Nucl. Mater.*, **275**, 28 (1999).

[5] H.P. Kim, S.S. Hwang, J.S. Kim and J.H. Hwang, "Stress corrosion cracking of steam generator tubing materials in lead containing solution," *Proc. of the 13th Int. Conf. on Environmental Degradation of Materials in Nuclear Power Systems*, Whistler, Canada, Aug. 19-23, 2007.

[6] D.J. Kim, H.C. Kwon and H.P. Kim, "Effects of the solution temperature and the pH on the electrochemical properties of the surface oxide films formed on Alloy 600," *Corros. Sci.*, **50**, 1221 (2008).

[7] S.W. Kim and H.P. Kim, "Electrochemical noise analysis of PbSCC of Alloy 600 SG tube in caustic environments at high temperature," *Corros. Sci.*, **51**, 191 (2009).

[8] J. Stewart, D. B. Wells, P. M. Scott and D. E. Williams, "Electrochemical noise measurements of stress corrosion cracking of sensitised austenitic stainless steel in high-purity oxygenated water at 288 °C," *Corros. Sci.*, **33**, 73 (1992).

[9] R.A. Cottis, M.A.A. Al-Awadhi, H. Al-Mazeedi and S. Turgoose, "Measures for the detection of localized corrosion with electrochemical noise," *Electrochim. Acta*, **46**, 3665 (2001).

[10] R.A. Cottis, "Interpretation of electrochemical noise data," *Corrosion*, **57**, 265 (2001).

[11] H.A.A. Al-Mazeedi and R.A. Cottis, "A practical evaluation of electrochemical noise parameters as indicators of corrosion type," *Electrochim. Acta*, **49**, 2787 (2004).

[12] J.M. Sanchez-Amyay, R.A. Cottis and F.J. Botana, "Shot noise and statistical parameters for the estimation of corrosion mechanisms," *Corros. Sci.*, **47**, 3280 (2005).

[13] K.H. Na, S.I. Pyun and H.P. Kim, "Analysis of electrochemical noise obtained from pure aluminium in neutral chloride and alkaline solutions," *Corros. Sci.*, **49**, 220 (2007).

[14] K.H. Na and S.I. Pyun, "Effects of sulphate, nitrate and phosphate on pit initiation of pure aluminium in HCl-based solution," *Corros. Sci.*, **49**, 2663 (2007).

[15] K.H. Na, S.I. Pyun and H.P. Kim, "Effects of NiB, PbO, and TiO_2 on SCC of sensitized Inconel Alloy 600 in RT-tetrathionate solution," *J. Electrochem. Soc.*, **154**, C349 (2007).

[16] U.C. Kim, K.M. Kim and E.H. Lee, "Effects of chemical compounds on the stress corrosion cracking of steam generator tubing materials in a caustic solution," *J. Nucl. Mater.*, **341**, 169 (2005).